A novel frequency response analysis model applicable to high-penetration wind power grid

Available online at www.sciencedirect.com
ScienceDirect
Energy Reports 8 (2022) 412–421
www.elsevier.com/locate/egyr

The 5th International Conference on Electrical Engineering and Green Energy, CEEGE 2022, 8–11 June, Berlin, Germany

A novel frequency response analysis model applicable to high-penetration wind power grid

Yi Hu[a,*], Zheng Wang[a], Tao Huang[b], Qingzhu Zeng[a]

[a] School of Electrical and Electronic Information, Xihua University, Chengdu 610039, China
[b] Department Ingegneria Elettrica, Politecnico Di Torino, Torino 10129, Italy

Received 22 July 2022; accepted 6 August 2022
Available online 19 August 2022

Abstract

The decoupling relationship and low inertia characteristics of wind turbine generator system (WTGS) make the system frequency response more complex. In order to evaluate the frequency stability of high-penetration wind power grid, it is significant to establish an exactly frequency response analysis model. Due to the features of wide spatial distribution and large number of WTGS in the power grid, the wind speed and actual operating state faced by WTGS in different regions have obvious discrepancy, which makes the traditional frequency response models that merely considers the single operating state of WTGS have evident limitations. Therefore, in order to consider the discrepancy of frequency regulation characteristics caused by the spatial dispersion of WTGS, an improved frequency response modeling method which can take into account the frequency regulation characteristics of multiple wind speeds is proposed. This method uses small signal analysis theory and fuzzy control method to construct an improved equivalent aggregation model of WTGS. Combining this model with the typical system frequency response (SFR) model, a novel frequency response model considering different wind conditions and different frequency regulation characteristics of WTGSs is established. Finally, an improved IEEE-118 bus system is used for case analysis to verify the correctness and superiority of the proposed method for high-penetration wind power grid.

Peer-review under responsibility of the scientific committee of the 5th International Conference on Electrical Engineering and Green Energy, CEEGE, 2022.

Keywords: High-penetration wind power grid; Frequency response model; Small signal analysis; SFR; Frequency regulation characteristics

1. Introduction

With the transformation of global energy consumption to renewable energy, the share of wind power has significantly increased year by year [1]. According to the relevant data, the global installed capacity of new wind power in 2020 was 93GW, a substantial increase of 52.96% compared with 2019. By the end of 2020, the global cumulative installed capacity of wind power has reached 742GW, including 707GW of onshore wind power and 35GW of offshore wind power [2]. Wind power has become one of the major energy sources around the world.

* Corresponding author.
E-mail address: 1220200001@mail.xhu.edu.cn (Y. Hu).

https://doi.org/10.1016/j.egyr.2022.08.097

Peer-review under responsibility of the scientific committee of the 5th International Conference on Electrical Engineering and Green Energy, CEEGE, 2022.

With the increasing penetration of wind power generation in modern power system, the strong randomness and low inertia of wind power have brought severe challenges to the frequency stability of the power grid [3]. In traditional power system, due to the relative decoupling relationship between spinner velocity of the WTGS and the system frequency, the influence of frequency regulation generally not be considered for small installed capacity and low rotational inertia WTGS [4,5]. However, when the massive-scale wind power is connected, in order to ensure the safe and stable operation of the power grid, it puts forward clear frequency regulation requirements to WTGS. At this time, the frequency regulation characteristics of WTGS must be considered in the frequency response analysis [6]. Therefore, a frequency analysis model of wind power grid is proposed in [7], which considering the inertia response of WTGS. Furthermore, a frequency response model considering the combined effects of inertia response with droop response of WTGS is discussed in [8], which improving the frequency estimation accuracy for wind power grid. A reduced-order WTGS model with primary frequency control is described in [9], which is combined with the SFR model to simulate the dynamic frequency of wind power grid. Although the frequency analysis models proposed in the above studies take into account the frequency regulation effect of WTGS, they mostly consider the frequency regulation ability of WTGS in a single operation state, and do not fully consider the frequency regulation characteristics of WTGSs in different operation state of the high-penetration wind power grid.

At present, the WTGS generally achieves deloading operation by adding virtual inertial control, over-speed-based deloading control, pitch angle control and other methods, and the frequency regulation effect produced by different deloading control methods will also be significantly different [10]. Considering the large quantity and extensive distribution of WTGSs in the high-penetration wind power grid, the WTGS in different regions will face different wind speed conditions. This leads to different control means of WTGS under different wind speed conditions, operating in different states and having different frequency modulation effects on the power system. Therefore, for the high-penetration wind power grid, the difference of frequency regulation characteristics caused by the spatial dispersion of WTGSs cannot be ignored. The need for establishing a frequency response model that can simultaneously consider different wind speed conditions and different frequency regulations has more significance. In this regard, Ref. [11] adds a wind speed determination module through logical judgment, and takes the average value of wind speeds to consider the influence of wind speed differences in the power grid. This method makes up for the influence of wind speed differences to the frequency response model to a certain extent. However, this method cannot accurately reflect the frequency characteristics of the system with high wind power penetration and wide dispersion area.

In view of the following limitations of the current research on the frequency response analysis of high-penetration wind power grid: (1) Few studies consider the difference of frequency regulation over different wind speeds and the combined effects on the frequency response characteristics; (2) The current frequency response model lacks flexibility tuning method of frequency regulation coefficient, which is not conducive to the equivalent accuracy of WTGS frequency regulation. This paper proposes an improved frequency dynamic response model for the high-penetration wind power grid. The proposed model simultaneously takes into account the disparate deloading control methods adopted by the WTGS under low, medium and high wind speeds, such as virtual inertial control, over-speed-based deloading control, pitch angle control and so on. Based on the theory of small signal analysis theory, the equivalent models of WTGS in different wind speeds operation areas are deduced by using wind kinetic energy equations and rotor motion equations. Meanwhile, the droop response coefficient in the virtual inertia control mode is tuned by adopting fuzzy control method, which ensures that the proposed model can more precisely reflect the actual frequency regulation effect.

2. Frequency response modeling ideas for high-permeability wind power grid

Considering that in the high-penetration wind power grid, WTGSs with different spatial distribution will face different wind speed conditions, which will have different frequency regulation effects. Therefore, based on the traditional SFR model, this paper proposes an equivalent aggregation model of frequency response analysis that can consider the existence of low, medium and high wind speeds simultaneously.

The main idea of the proposed model is that the traditional generators and loads are still equivalent to the SFR model, and then the small-signal analysis means is adopted to process the state equation of the WTGS which regards the wind speed as a small signal interference. Due to the differences of WTGS control models operate at different wind speed conditions, the establishment of the model should consider the different components of the power equation at the specific operating point. Finally, based on the difference of power equation, the WTGS

equivalent model of two inputs and single output considering different wind conditions will be obtained. Thus, the frequency response equivalent model of high-penetration wind power grid can be obtained as Fig. 1.

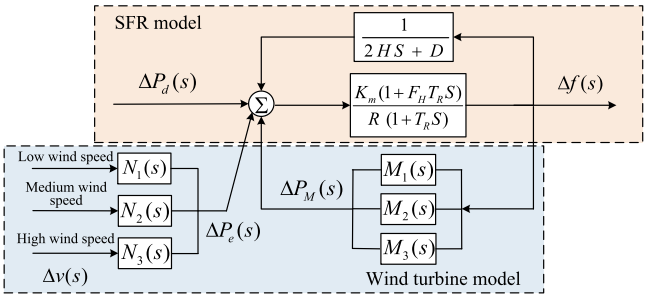

Fig. 1. The equivalent model of the high-penetration wind power grid.

In the frequency response model, Δf is the variation value of frequency, H represents the aggregate inertia time constant of all generators, D represents the aggregate damping coefficient of the power system, K_m is mechanical power gain, T_R represents the reheating time constant in prime mover system, F_h represents the proportion of output power in high-pressure cylinder, R is the governor adjustment coefficient, $M_1(s)$, $M_2(s)$ and $M_3(s)$ represent the transfer function between electromagnetic power change $\Delta P_e(s)$ and $\Delta f(s)$, $N_1(s)$, $N_2(s)$ and $N_3(s)$ represent the transfer function of power change caused by wind speeds, $\Delta P_M(s)$ represents the frequency regulation power, $\Delta P_d(s)$ and $\Delta v(s)$ represent the load disturbance and wind speed disturbance of the power grid.

3. The equivalent models of WTGSs in different wind conditions

3.1. Modeling of frequency regulation characteristics at low wind speed

When the WTGS operates at low wind speed condition, the spare rotational kinetic energy of WTGS is much low. Therefore, the virtual inertial control of the WTGS should not be considered, and the WTGS does not provide frequency support when operating at this wind condition [12]. Accordingly, the transfer function of inertial response part should not exist.

On the basis of the aerodynamic principle, the wind energy obtained by the WTGS can be expressed as [12]:

$$P_m = \rho\pi r^2 v^3 C_p / 2P_{wb},\ C_P = C_P(\lambda, \beta) \tag{1}$$

where ρ is the air mass density; r is the wind wheel radius; λ is tip velocity ratio; β is pitch angle of WTGS; C_p is the utilization coefficient of wind power, which is a function between β and λ; P_{wb} is the rated power.

C_p and λ reflect the operation state of the WTGS, which can be expressed as

$$C_P = P/0.5\rho v^3 s = 2Tw/\rho v^3 s = P/0.5\rho v^3 s = (Tw)/0.5\rho v^3 s = (\lambda * T)/0.5\rho v^2 s = K_c\lambda \tag{2}$$

where P represents the actual captured power; s is the swept area of the wind wheel; T is the mechanical torque of the actual power; w represents angular velocity of wind wheel; K_c is the relationship coefficient.

Assuming that the proportion of WTGS capacity operating at low wind speed at a certain time is K_1, the rotor swing equation of WTGS can be obtained as

$$\Delta T_M(s) - \Delta T_E(s) = T_J K_1 s \Delta w(s) = 2H_W K_1 s \Delta w(s) \tag{3}$$

$$\Delta P_M = K_{de} * (\rho\pi r^2 v^3 C_p)/(2P_{wb}) \tag{4}$$

The load deloading method of low wind speed operation is to change the rotor speed. The mechanical torque at a certain point can be expressed by the partial derivative of w and v, which can be obtained as

$$\Delta T_M(s) = (\partial T_M)/(\partial f) * \Delta f(s) + (\partial T_M)/(\partial w) * \Delta w(s) + (\partial T_M)/(\partial v) * \Delta v(s) \tag{5}$$

The mechanical power torque increment can be obtained by combining the above equations:

$$\Delta T_M(s) = [(K_w K_c v^3\lambda - K_w v^3 C_p)/(w^2)] * \Delta w(s) + [(3K_w C_p v^2 - K_w K_c v^2\lambda)/(w)] * \Delta v(s) \tag{6}$$

where K_w is virtual inertia control coefficient; K_p is droop coefficient.

When the WTGS operates at low wind speed condition, the virtual inertial integrated control function of the WTGS is not considered, the electromagnetic power change of the WTGS is only caused by the wind speed changing, then the electromagnetic torque can be written as

$$\Delta P_e(s) = \Delta T_E(s) * \Delta w(s) \tag{7}$$

Putting Eqs. (5) and (6) into Eq. (7), the frequency change can be obtained as

$$\Delta w(s) = \{[K_w v^2 w(3C_{pref} + K_c\lambda)]/[K_w v^3(K_c\lambda - C_{pref}) - 2K_p w^3 - 2K_c H_w s w^2]\} * \Delta v(s) \tag{8}$$

Therefore, the electromagnetic power can be obtained by the electromagnetic power torque of the WTGS and Eq. (8).

$$\Delta P_e(s) = \{[2K_P K_1 K_w v^2 w^2(3C_p + K_c\lambda)]/[K_w v^3(K_c\lambda - C_p) - 2K_p w^3 - 2K_c H_w s w^2]\} * \Delta v(s) \tag{9}$$

Through the above analysis, the transfer function of the WTGS equivalent model at low wind speed condition can be described as

$$M_1(s) = [2K_1 K_P K_w v^2 w^2(3C_{pref} + K_c\lambda)]/[K_w v^3(K_c\lambda - C_{pref}) - 2K_p w^3 - 2K_c H_w s w^2] \tag{10}$$

$$N_1(s) = 0 \tag{11}$$

3.2. Modeling of frequency regulation characteristics at medium wind speed

When the WTGS is operating at medium wind speed and possessing sufficient rotational reserve, the virtual inertial control should be considered and the rotor kinetic energy recovery method should be adopted. When the output-power of the WTGS is less than the rated value, the pitch angle remains unchanged at about 0 degree and the output-power is add by adjusting the rotor speed. The principle of pitch angle control method is that the operating point is moved from the maximum to another stable operating point by augmenting pitch angle of WTGS to restore the reserve power [12]. Therefore, the over-speed-based deloading control meets the load reduction requirements in medium wind speed.

The maximum mechanical power of the WTGS can be expressed as

$$P_{opt} = (\rho\pi r^2 v^3 C_{p\max})/(2P_{wb}) \tag{12}$$

where P_{opt} is the operating power of WTGS; $C_{p\max}$ is the maximum value of C_p.

By adjusting the speed of the WTGS, there is a unique tip velocity ratio can maximize C_p. According to the principle of over-speed-based deloading and pitch angle control, the deloading reserve power can be described as:

$$P_{de} = K_{de} K_w {w_{opt}}^3 \tag{13}$$

$$P_{res} = P_{opt} - P_{de} = (\rho s v^3 C_p)/2 = 1 - K_{de} P_{opt} \tag{14}$$

where P_{de} is the deloading power; P_{res} is the active output-power after deloading; P_{opt} is the output-power before deloading; K_{de} is the deloading coefficient, reflecting the level of actual deloading.

According to the output-power curve and the triangular similarity theorem, the actual output-electromagnetic-power of a certain operating point can be obtained as:

$$P_e = P_{de} + (P_{opt} - P_{de}) w'_{de} = P_{de} + (P_{opt} - P_{de}) w'_{de} \tag{15}$$

where w_{de} is the angular velocity of WTGS after deloading; $w_{\max}$ is the angular velocity before deloading.

According to the deloading method, the mechanical torque at a certain point can be expressed by the partial derivative of rotational speed, wind speed, tip velocity ratio and pitch angle (when the spinner velocity is low, the partial derivative of torque angle is 0):

$$\Delta T_M(s) = (\partial T_M)/(\partial w) * \Delta w(s) + (\partial T_M)/(\partial v) * \Delta v(s) + (\partial T_M)/(\partial \lambda) * \Delta\lambda(s) + (\partial T_M)/(\partial \beta) * \Delta\beta(s) \tag{16}$$

The tip velocity ratio equation obtained based on small signal analysis and the simplified form can be described as

$$\lambda + \Delta\lambda(s) = (w + \Delta w(s))/(v + \Delta v(s)) \tag{17}$$

The change of electromagnetic power torque caused by the virtual inertia control of WTGS can be described as

$$T_E(s) = (1 - K_{de})K_w w^2 w'_{de} + K_{de}K_w w^2 - [(1/R_v + K_p s)/w] * \Delta f(s) \tag{18}$$

where R_v is integrated virtual control coefficient.

Substituting Eqs. (14) and (15) into Eq. (16), and the change value of mechanical power torque can be obtained as

$$\Delta T_M(s) = 3K_w {w_{opt}}^2 \Delta w(s) + 6K_w v^2 C_p \Delta v(s) + K_w r^2 v^3 * [T/(0.5\rho v^2 s)] * \Delta f(s) \tag{19}$$

For medium wind speed conditions, it is assumed that the proportion of WTGS capacity is K_2. The swing equation of the WTGS and the frequency regulation output-power of WTGS (ΔP_{T2}) can be described as

$$\Delta T_M(s) - \Delta T_E(s) = 2K_2 H_w s \Delta w(s) \tag{20}$$

$$\Delta P_{T2}(s) = \Delta P_M(s) + \Delta P_E(s) = N_2(s)\Delta v(s) + M_2(s)\Delta f(s) \tag{21}$$

Combining the Eq. (19), (20) and Eq. (21), the transfer function of the equivalent model at medium wind speed can be obtained as

$$M_2(s) = a_2/(b_2 s + 1) \tag{22}$$

$$N_2(s) = -(c_2 s^2 + d_2 s + e_2)/(b_2 s + 1) \tag{23}$$

where $a_2 = [3(1 - K_{de})K_w w^2 + 3K_{de}K_w w^2 w'_{de} - (K_{de}K_w w^3)/(w_{de} - w_{\max})][3K_w w v^2 C_p - K_w K_c w v^2 \lambda]/f_2$, $b_2 = 2K_2 H_w w^2/f_2$, $c_2 = 2K_2 H_w K_p w^2/f_2$, $d_2 = [2K_2 H_w w^2/R_v + K_p v^3 C_p - (1 - K_{de} - K_2)K_p K_w w^3 - K_{de}K_w K_p w^3 w'_{de} - K_{de}K_w K_p w^2]/f_2$, $e_2 = [K_w K_2 H_w v^3 C_p/R_v - (1 - K_{de})K_w w^3/R_v - K_2 K_w K_p w v^2/R_v - K_{de}K_w K_p w^2 w'_{de}]/f_2$, $f_2 = 2(1 - K_{de})K_w w^3 + K_w v^3 C_p + 2K_{de}K_w w^3 w'_{de} - (K_{de}K_w w^4)/(w_{de} - w_{\max}) - K_w K_c w v^2$.

3.3. Modeling of frequency regulation characteristics at high wind speed

When the WTGS is operating at high wind speed, the speed of the rotor would reach the setting rated value. For the safe and stable operation of the WTGS, it not applicable to change the output-power only by adjusting the speed of the rotor. Therefore, the deloading method of changing the pitch angle is selected in the high wind speeds. By altering the windward blades angle, the input mechanical power of the WTGS can be changed to making the WTGS operates at a certain operating state, leaving a certain reserve power to support the possible power shortage of the wind power grid.

On basis of aerodynamic principle, the output-power of the WTGS can be described as

$$P_{opt} = (\rho \pi r^2 v^3 C_{p\max}(\beta_0))/(2P_{wb}) = k {w_{\max}}^3 \tag{24}$$

where β_0 is the actual pitch angle value.

According to the principle of pitch angle deloading control, the variable of pitch angle can be expressed as

$$\Delta\beta = D_b \Delta f \tag{25}$$

where D_b is the changing coefficient of pitch angle.

The pitch angle equation based on small signal analysis and its simplified form can be described as

$$\beta + \Delta\beta(s) = (w + \Delta w(s))/(v + \Delta v(s)) \tag{26}$$

At high wind speed, the change of mechanical torque at a certain operating point of the WTGS can be expressed by the rotational speed, wind speed, tip velocity ratio and the partial derivative of pitch angle, which can be described as

$$\Delta T_M(s) = (\partial T_M)/(\partial w) * \Delta w(s) + (\partial T_M)/(\partial v) * \Delta v(s) + (\partial T_M)/(\partial \lambda) * \Delta\lambda(s) + (\partial T_M)/(\partial \beta) * \Delta\beta(s) \tag{27}$$

Combined with Eqs. (25) and (26), the change value of the electromagnetic torque can be obtained as

$$T_E(s) = (1 - K_{de})K_w w^2 w'_{de} + K_{de}K_w w^2 - [(1/R_v + K_v s)/w] * \Delta f(s) \tag{28}$$

For high wind speed conditions, it is assumed that the proportion of WTGS capacity is K_3. The swing equation of the WTGS can be expressed as

$$\Delta T_M(s) - \Delta T_E(s) = 2K_3 H_w s \Delta w(s) \tag{29}$$

Substituting Eqs. (27) and (28) into Eq. (29), the frequency change and the frequency regulation output-power of WTGS (ΔP_{T3}) can be obtained as

$$\Delta w(s) = [K_w v^2 w(3C_p + K_c\lambda) - 2Kp H_w s w]/[K_w v^3(K_c\lambda - C_p) - 2K_p w^3 - 2K_c H_w s w^2] * \Delta v(s) \tag{30}$$

$$\Delta P_{T3}(s) = \Delta P_M(s) + \Delta P_E(s) = N_3(s)\Delta v(s) + M_3(s)\Delta f(s) \tag{31}$$

The transfer function of the equivalent models at high wind speed can be written as

$$M_3(s) = a_3/(b_3 s + 1) \tag{32}$$

$$N_3(s) = -(c_3 s^2 + d_3 s + e_3)/(b_3 s + 1) \tag{33}$$

where $a_3 = (2K_3 H_w w^2 + 1/R_v)/f_3$, $b_3 = [3K_3 H_w w^2(3C_p - K_c\lambda) + D_b v^2]/f_3$, $c_3 = (3K_3 H_w w^2 K_p)/f_3$, $d_3 = (3K_3 H_w w^2/R_v - 3K_3 K_w K_p w^2 + 2K_p K_w D_b w^3 - K_p w v^2 - 1/R_v)/f_3$, $e_3 = [(2K_3 K_w w^3 - 2K_p K_w w^3 + K_3 K_w v^3 C_p)/R_v - (3w^2 D_b)/R_v]/f_3$, $f3 = 2K_w w^3 + K_w v^3 C_p - K_3 K_w K_c w v^2$.

4. Tuning the droop response coefficient of WTGS

According to the previous analysis, WTGSs contribute differently to the frequency regulation in the face of different wind speeds. Therefore, seeking the appropriate frequency regulation coefficient has far-reaching significance to improve the accuracy of frequency response [13]. In this section, the droop response coefficients are obtained by using fuzzy control theory, which is mainly based on the WTGS operating conditions and the frequency response results. Finally, comparing the output-power difference value of WTGS with the setting threshold to estimate whether the WTGS renew to MPPT operation state.

The purpose of this section is to obtain the droop response coefficient that can most accurately reflect the frequency regulation effect of the actual WTGSs through the improved fuzzy control method, and improve the accuracy of the frequency response model. The method is seeking the frequency regulation through fuzzy control theory, the input-quantity of fuzzy control are the frequency difference and the frequency change rate, the domain of input are set as [0,1] and limiting range of limiters is [-0.2,0.2], [0,1]. The output of the fuzzy controller is Kf (the droop response coefficient of WTGS) and the domain of output is [-0.125,0.875]. In the fuzzy control model, the input and output are described in 9, 6 and 9 kinds of fuzzy languages respectively. The fuzzy control rules are established as follows: when the wind power penetration is high and frequency recovers slowly, slow down the speed of wind power recovers by reducing Kf; when the wind power penetration is high and frequency recovers fastly, forcing the speed of wind power recover by increasing Kf; when the wind power penetration is low and frequency recovers is too fast, the speed of wind power recovery can be accelerated by increasing Kf [14] (see Fig. 2).

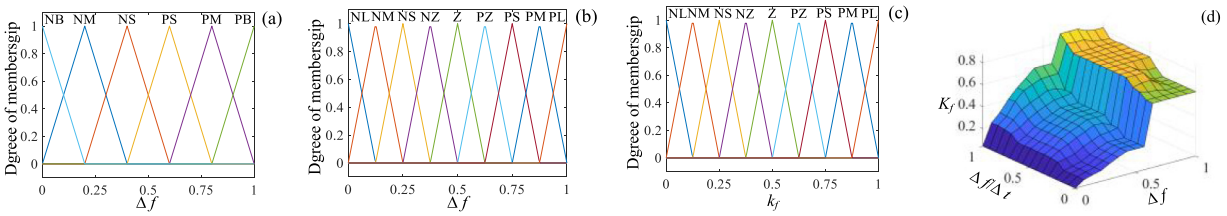

Fig. 2. The fuzzy controller. (a) input of fuzzy controller; (b) input of fuzzy controller; (c) output of fuzzy controller; (d) output of fuzzy controller.

5. Case study

5.1. Introduction to simulation system

In this paper, the IEEE-118 node system is improved [12]. The improved system includes 14 conventional generators and 40 WTGSs, of which all the conventional generators are equipped with governors and can participate

in primary frequency control. The role of frequency control should be also required for all WTGSs. In this section, PSSE is used to establish the time-domain simulation model of the improved system, so as to carry out simulation analysis and verify the accuracy of the improved frequency response model.

Among the simulation analysis, the wind speed levels are set as follows: When the wind speed v_m satisfies $0 \leq v_m \leq 5$ m/s, the WTGS operates at the low wind speed area; When the wind speed satisfies $5 < v_m \leq 12$ m/s, the WTGS operates at the medium wind speed area; When the wind speed satisfies $12 < v_m \leq 16$ m/s, the WTGS operates at the high wind speed area. The cut-in wind speed of the WTGS is set as 3 m/s, and the cut-out wind speed is set as 16 m/s.

For convenience of expression, in all the following cases, the proposed improved frequency response model is labeled as IM, the conventional frequency response model proposed in [11] is labeled as CM, and the time-domain simulation model of PSSE is labeled as TDSM.

5.2. Analysis of simulation

- *The frequency response analysis under power* shortage and *wind speed changing*

Condition 1. It is set that the wind speed in each region of the power system remains basically unchanged during the disturbance period. At this moment, the low wind speed is 6.5 m/s, medium wind speed is 10.5 m/s and high wind speed is 12.5 m/s. The number of WTGSs operating at low, medium and high wind speed are 14, 14 and 12 respectively, and the penetration of the wind power system is 60%. When $T = 5$ s, the load has a power shortage of 20%, and the value of droop response coefficient calculated by fuzzy control algorithm is 0.42.

The post-disturbance frequency dynamic curves and the additional power of WTGSs calculated by IM and CM are compared with the simulation results of TDSM, as shown in Fig. 3.

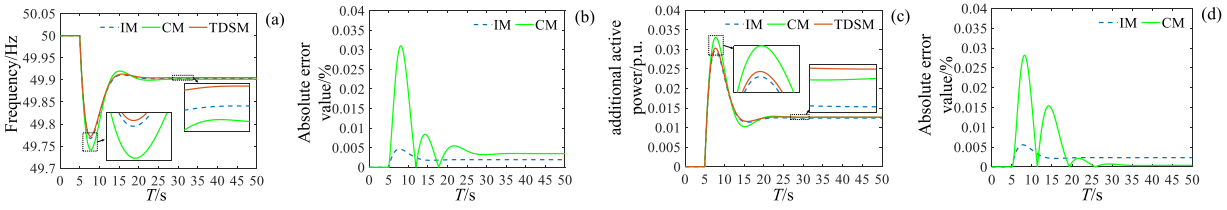

Fig. 3. Comparisons of the frequency response between IM and CM in the condition of power shortage. (a) system frequency; (b) frequency error; (c) additional active power; (d) active power error.

In order to further compare the prediction effects of IM and CM, the numerical comparison is made for the key characteristic values of the frequency response curves in Fig. 3 respectively. The results are listed in Table 1 below:

Table 1. Comparison results of frequency characteristic values.

Model	Lowest frequency		Steady-state frequency	
	Value/HZ	Absolute error/%	Value/Hz	Absolute error/%
IM	49.768	0.005	49.921	0.004
CM	49.738	0.032	49.929	0.002
TDSM	49.764	/	49.923	/

By comparing frequency response curves in Fig. 3 and the key characteristic values in Table 1, it can be seen that for the same disturbance, the lowest frequency value of IM is 49.768 Hz and the steady-state frequency value is 49.921 Hz, while the results of CM are 49.738 Hz and 49.929 Hz respectively. Therefore, the frequency response of IM has higher prediction accuracy than CM, which is closer to simulation results of TDSM. It is verified that the proposed model can more accurately and effectively analyze the frequency response characteristics of the high-penetration wind power grid.

Condition 2. It is set that there is no power disturbance in the system, but the wind speed is changed. When T=3s, due to the weather abruptly change of the wind power grid, the wind speed decreases by 2 m/s, and the other operating parameters are the same as Condition 1.

At this time, the proposed model (IM) and the conventional model (CM) are also used to analyze the frequency response after disturbance, and the comparison of frequency response curves is shown in Fig. 4.

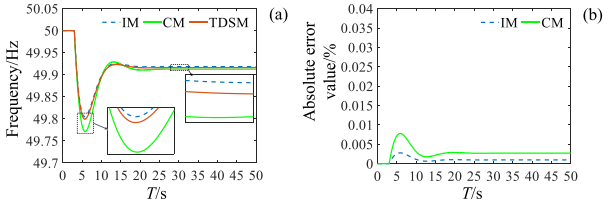

Fig. 4. (a) system frequency; (b) the absolute error.

This simulation results first fully show that the influence of the wind speed change on the power grid frequency cannot be ignored. In addition, through the comparison of Fig. 4, it can be proved that IM can more accurately reflect the frequency regulation characteristics of the WTGSs under different wind speeds, which has obvious advantages over CM.

• *The analysis of frequency response model under different wind power penetration*

The frequency response analysis model proposed in this paper is mainly aimed at the frequency analysis of high-penetration wind power grid, so it is necessary to proved the accuracy of the model under different penetration rates. The system conditions of this case are set to be the same as Condition 1 of the Case 1, and merely the wind power penetration rate of the system is changed to 30%, 40%, 65%, and 70%, respectively. When T=5s, the load has a power shortage of 20%, and the droop response coefficient is set as 0.42. The response results of IM and CM on the frequency and the absolute errors are compared with the results of TDSM, which are shown in Fig. 5.

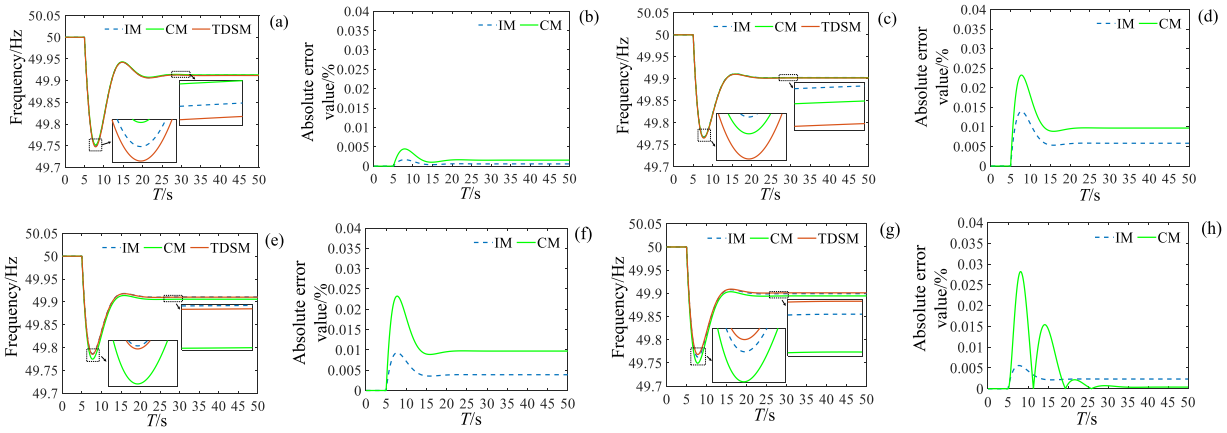

Fig. 5. Frequency response under different penetration rates. (a) system frequency (30%); (b) frequency error (30%); (c) system frequency (40%);(d) frequency error (40%); (e) system frequency (65%); (f) frequency error (65%); (g) system frequency (70%); (h) frequency error (70%).

In order to highlight the applicability of the proposed model, the frequency key characteristic values and absolute errors obtained by the two models under different wind power penetration are compared. The results are listed in Table 2 below:

Through the comparison results of Fig. 5 and Table 2, it can be aware that the effect of the proposed model will be different with the discrepancy of wind power penetration. When the penetration rate is 30% and 40%, the absolute errors of the proposed model reduced with the wind power penetration increased, the calculation result of the IM is closer to the result of TDSM than the CM, but its advantage is not obvious. When the wind power penetration rate

Table 2. Comparison of frequency characteristic values and errors under different penetration rates.

Penetration rates/%	Lowest frequency					Steady-state frequency				
	IM		CM		TDSM	IM		CM		TDSM
	Value/Hz	Absolute error/%	Value/Hz	Absolute error/%	Value/Hz	Value/Hz	Absolute error/%	Value/Hz	Absolute error/%	Value/Hz
30	49.7986	0.05	49.7986	0.02	49.7984	49.9289	0.08	49.9314	0.024	49.9312
40	49.7648	0.013	49.7665	0.024	49.7668	49.9038	0.014	49.9048	0.023	49.9046
65	49.7854	0.01	49.7862	0.023	49.7853	49.9085	0.09	49.9112	0.023	49.9098
70	49.718	0.04	49.7453	0.032	49.7453	49.9036	0.02	49.9048	0.046	49.9042

increases to 65% and 70%, the absolute error of proposed model reduce to 0.023% and 0.02% respectively, which illustrate that the accuracy of the IM is significantly improved and the accuracy advantage is more obviously. It is verified that the proposed model is more suitable for high-penetration wind power grid than low-penetration wind power grid, and its advantages will be more significant with the increase of wind power penetration.

•*The analysis of frequency response model under different WTGS proportion*

The proportion of WTGSs under different wind speeds is an important parameter affecting the frequency response model. For illustrating its impact on the prediction effect of frequency response, the system operating condition in this case is the same as Condition 1 in the Case 1. Only the number of WTGSs under low, medium and high wind speed conditions are changed, and three schemes are set according to different proportions. In scheme 1, the number of WTGSs operating at low, medium and high wind speeds are 10, 22 and 8 respectively; In scheme 2, the numbers are 14, 14 and 12, and in scheme 3, the numbers are 10, 12 and 18.

Through the three schemes, the frequency response results of the IM and CM are compared with TDSM, and the absolute error curves are calculated, which are shown in Fig. 6.

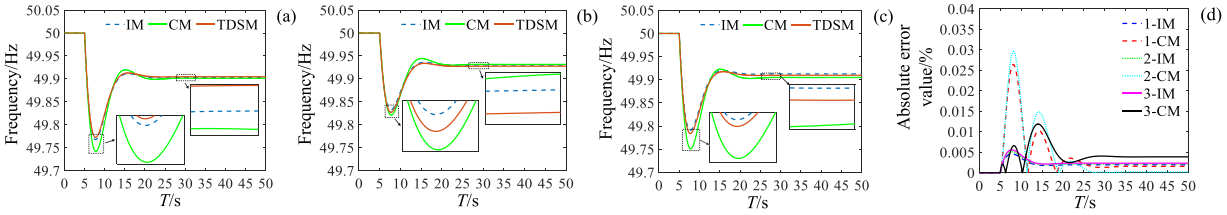

Fig. 6. Frequency results and absolute error of the three schemes. (a) system frequency of scheme 1; (b) system frequency of scheme 2; (c) System frequency of scheme 3; (d) frequency error.

According to the comparison results shown in Fig. 6, although IM has more advantages over CM on the whole, it is obvious that when the proportion of WTGSs in the three wind speeds is close, the accuracy advantage of IM is relatively small compared with CM, and when the proportion of WTGSs in the three wind speeds is quite different, the accuracy advantage of IM is more obvious than CM. This verifies once again that IM can simultaneously take into account the different frequency regulation characteristics of WTGSs under various wind speeds, and is more suitable for frequency response analysis of the high-penetration wind power grids with wide distribution of wind farms and significant regional wind speed differences.

6. Conclusion

In order to obtain a more accurate frequency response model for high-penetration wind power grid, this paper first establishes the equivalent model of WTGS frequency regulation characteristics under different wind conditions based on the swing equation and small signal analysis theory, and uses fuzzy control algorithm to find the appropriate frequency droop response coefficient. Then, based on the traditional SFR model, the frequency response analysis model suitable for high-penetration wind power grid is constructed. Finally, the improved IEEE-118 node system is used for verification and simulation analysis. The results of case studies show that the proposed model can exactly

reflect the frequency response characteristics of the high-penetration wind power grid, and has more advantages in accuracy than the conventional model. More importantly, this advantage becomes more obvious with the augment of wind power penetration and wind speed difference in the power grid.

Declaration of competing interest

The authors declare that they have no known competing financial interests or personal relationships that could have appeared to influence the work reported in this paper.

Data availability

Data will be made available on request.

Acknowledgments

This work was supported by the Talent Introduction Project of Xihua University (Z201035).

References

[1] Zin AABM, HA MP, Khairuddin AB, et al. An overview on doubly fed induction generators ′ controls and contributions to wind based electricity generation. Renew Sustain Energy Rev 2013;27:692–708, 2013.
[2] Khan FH, Pal T, Kundu B, et al. Wind energy: A practical power analysis approach. In: 2021 innovations in energy management and renewable resources, no. 52042. IEEE; 2021, p. 1–6, 2021.
[3] Ye Y, Qiao Y, Lu Z. Revolution of frequency regulation in the converter-dominated power system. Renew Sustain Energy Rev 2019;111:145–56, 2019.
[4] Hussain J, Mishra MK. An efficient wind speed computation method using sliding mode observers in wind energy conversion system control applications. IEEE Trans Ind Appl 2019;56(1):730–9, 2019.
[5] Tsili M, Papathanassiou S. A review of grid code technical requirements for wind farms. IET Renew Power Gener 2019;3(3):308–32, 2019.
[6] Boyle J, Littler T, Foley AM. Frequency regulation and operating reserve techniques for variable speed wind turbines. In: 2021 IEEE madrid power tech. IEEE; 2021, p. 1–5, 2021.
[7] Lee Dong-Jing, Wang Li. Small-signal stability analysis of an autonomous hybrid renewable energy power generation/energy storage system Part I: Time-domain simulations. IEEE Trans Energy Convers 2008;23(1):311–20, 2008.
[8] Rebello E, Watson D, Rodgers M. Performance analysis of a 10 MW wind farm in providing secondary frequency regulation: Experimental aspects. IEEE Trans Power Syst 2019;34(4):3090–7, 2019.
[9] Rebello E, Watson D, Rodgers M. Performance analysis of a 10 MW wind farm in providing secondary frequency regulation: Experimental aspects. IEEE Trans Power Syst 2019;34(4):3090–7, 2019.
[10] Li W, Chao P, Liang X, et al. A practical equivalent method for DFIG wind farms. IEEE Trans Sustain Energy 2017;9(2):610–20, 2017.
[11] Dai J, Tang Y, Wang Q, et al. An extended SFR model with high penetration wind power considering operating regions and wind speed disturbance. IEEE Access 2019;7:103416-103426, 2019.
[12] Subburaj AS, Bayne SB, Giesselmann MG, et al. Analysis of equivalent circuit of the utility scale battery for wind integration. IEEE Trans Ind Appl 2016;52(1):25–33, 2016.
[13] Bai K, Zou D, Zhang Z, et al. Digital mobile fronthaul based on performance enhanced multi-stage noise-Shaping Delta-sigma modulator. J Lightwave Technol 2020;39(2):439–47, 2020.
[14] Wang X, Xu B, Li S, et al. Composite learning fuzzy control of stochastic nonlinear strict-feedback systems. IEEE Trans Fuzzy Syst 2019;29(4):705–15, 2019.